Title	The surface-associated exopolysaccharide of Bifidobacterium longum 35624 plays an essential role in dampening host proinflammatory responses and repressing local TH17 responses
Authors	Schiavi, Elisa;Gleinser, Marita;Molloy, Evelyn;Groeger, David;Frei, Remo;Ferstl, Ruth;Rodriguez-Perez, Noelia;Ziegler, Mario;Grant, Ray;Moriarty, Thomas Fintan;Plattner, Stephan;Healy, Selena;O'Connell Motherway, Mary;Akdis, Cezmi A.;Roper, Jennifer;Altmann, Friedrich;van Sinderen, Douwe;O'Mahony, Liam
Publication date	2016-12
Original Citation	Schiavi, E., Gleinser, M., Molloy, E., Groeger, D., Frei, R., Ferstl, R., Rodriguez-Perez, N., Ziegler, M., Grant, R., Moriarty, T. F., Plattner, S., Healy, S., O'Connell Motherway, M., Akdis, C. A., Roper, J., Altmann, F., van Sinderen, D. and O'Mahony, L. (2016) 'The Surface-Associated Exopolysaccharide of Bifidobacterium longum 35624 Plays an Essential Role in Dampening Host Proinflammatory Responses and Repressing Local TH17 Responses', Applied and Environmental Microbiology, 82(24), pp. 7185-7196. doi:10.1128/aem.02238-16
Type of publication	Article (peer-reviewed)
Link to publisher's version	http://aem.asm.org/content/82/24/7185.abstract - 10.1128/aem.02238-16
Rights	© 2016, American Society for Microbiology. All Rights Reserved.
Download date	2023-05-07 19:25:11
Item downloaded from	http://hdl.handle.net/10468/5413

The surface associated exopolysaccharide of *Bifidobacterium longum* 35624 plays an essential role in dampening host pro-inflammatory responses and in repressing local TH17 responses

Running title: *B. longum* exopolysaccharide modulates TH17 responses

Elisa Schiavi[a,b], Marita Gleinser[c], Evelyn Molloy[c], David Groeger[b], Remo Frei[a], Ruth Ferstl[a], Noelia Rodriguez-Perez[a], Mario Ziegler[a], Ray Grant[b], Thomas Fintan Moriarty[d], Stephan Plattner[e], Selena Healy[e], Mary O'Connell Motherway[c], Cezmi A. Akdis[a], Jennifer Roper[e], Friedrich Altmann[f], Douwe van Sinderen[c], Liam O'Mahony[a#]

[a]Swiss Institute of Allergy and Asthma Research (SIAF), University of Zürich, Davos, Switzerland; [b]Alimentary Health Pharma Davos, Davos, Switzerland; [c]APC Microbiome Institute and School of Microbiology, University College Cork, Cork, Ireland; [d]AO Research Institute Davos, Davos, Switzerland; [e]Alimentary Health, Cork Ireland; [f]BOKU, Vienna, Austria

Running Head: Immunoregulation by bifidobacterial surface polysaccharide

#Address correspondence to Liam O'Mahony, liam.omahony@siaf.uzh.ch.

Abstract word count: 200

Manuscript word count: 5,926

ABSTRACT

The immune modulating properties of certain bifidobacterial strains, such as *Bifidobacterium longum* subsp. *longum* **35624™** (*B. longum* 35624), have been well described, although the strain-specific molecular characteristics associated with such immune regulatory activity are not well defined. It has previously been demonstrated that *B. longum* **35624** produces a cell surface exopolysaccharide and in this study we investigated the role played by this exopolysaccharide in influencing the host immune response. *B. longum* **35624** induced relatively low levels of cytokine secretion from human dendritic cells, whereas an isogenic exopolysaccharide-negative mutant derivative (termed sEPS^{neg}) induced vastly more cytokines, including IL-17, which was reversed when exopolysaccharide production was restored in sEPS^{neg} by genetic complementation. Administration of *B. longum* **35624** to the T cell transfer colitis model prevented disease symptoms, whereas sEPS^{neg} did not protect against the development of colitis, with associated enhanced recruitment of IL-17+ lymphocytes to the gut. Moreover, intra-nasal administration of sEPS^{neg} also resulted in enhanced recruitment of IL-17+ lymphocytes to the murine lung. These data demonstrate that the particular exopolysaccharide produced by *B. longum* **35624** plays an essential role in dampening pro-inflammatory host responses to the strain and that loss of exopolysaccharide production results in the induction of local T_H17 responses.

IMPORTANCE

Particular gut commensals, such as *B. longum* **35624**, are known to contribute positively to the development of mucosal immune cells, resulting in protection from inflammatory diseases. However, the molecular basis and mechanisms for these commensal-host interactions are poorly described. In this report, an exopolysaccharide was shown to be

decisive in influencing the immune response to the bacterium. We generated an isogenic mutant unable to produce exopolysaccharide, and observed that this mutation caused a dramatic change in the response of human immune cells *in vitro*. In addition, mouse models confirmed that lack of exopolysaccharide production induces inflammatory responses to the bacterium. These results implicate the surface-associated exopolysaccharide of the *B. longum* **35624** cell envelope in the prevention of aberrant inflammatory responses.

INTRODUCTION

The gut microbiota contributes significantly to host health via multiple mechanisms, including the digestion of foods, competitive exclusion of pathogens, enhancement of epithelial cell differentiation and promotion of mucosa-associated lymphoid tissue proliferation (1, 2). Furthermore, accumulating evidence suggests that the composition and metabolic activity of the gut microbiota has profound effects on proinflammatory activity and the induction of immune tolerance within mucosal tissue (3-5). Certain microbes induce regulatory responses, while others induce effector responses, resulting in the case of healthy individuals in a balanced homeostatic immunological state, which protects against infection and controls aberrant, tissue-damaging inflammatory responses (6).

One bacterial strain, which is known to induce tolerogenic responses within the gut, is *Bifidobacterium longum* subsp. *longum* **35624**™ (7). Induction of T regulatory (Treg) cells by the *B. longum* **35624** strain in mice is associated with protection against colitis, arthritis, allergic responses and pathogen-associated inflammation (8-12). Administration of this bacterium to humans increases Foxp3+ lymphocytes in peripheral blood, enhances IL-10 secretion *ex vivo*, and reduces the level of circulating proinflammatory biomarkers in a wide range of patient groups (13, 14). A number of host mechanisms have been described, which contribute to the anti-inflammatory activity of this microbe, including Toll-like receptor 2 (TLR-2) and Dendritic Cell-Specific Intercellular adhesion molecule-3-Grabbing Non-integrin (DC-SIGN) recognition, and retinoic acid release by dendritic cells (13, 15-17). However, the bacterial strain-specific structural and/or metabolic factors that contribute to these protective immune responses have as yet remained elusive.

71 A number of different exopolysaccharides from gut microbes have been shown to
72 induce immune-modulatory effects. Polysaccharide A (PSA) from *Bacteroides fragilis*
73 mediates the conversion of naïve $CD4^+$ T cells into $Foxp3^+$ Treg cells that produce IL-10
74 during commensal colonization. Functional Treg cells are also induced by PSA during
75 intestinal inflammation, which requires TLR-2 signaling (18). Further studies have reported
76 that PSA interacts directly with mouse plasmacytoid dendritic cells via TLR-2 and that PSA-
77 exposed plasmacytoid dendritic cells express molecules involved in protection against colitis
78 and stimulate $CD4^+$ T cells to secrete IL-10 (19). An exopolysaccharide from *Bacillus subtilis*
79 prevents gut inflammation stimulated by *Citrobacter rodentium*, which is dependent on TLR-
80 4 and MyD88 signaling (20). Similarly, protection against *C. rodentium* infection by
81 *Bifidobacterium breve* UCC2003 was dependent on the presence of its exopolysaccharide
82 (21). Furthermore, it was described that an extracellular polymeric matrix, isolated from
83 *Faecalibacterium prausnitzii*, displayed anti-inflammatory activity in the mouse dextran
84 sodium sulphate colitis model (22).

85 We recently described that the *B. longum* **35624** strain-specific EPS gene cluster,
86 designated as eps_{624}, is responsible for the production of a cell surface-associated
87 exopolysaccharide, composed of a branched hexasaccharide repeating unit with two
88 galactoses, two glucoses, galacturonic acid and the unusual sugar 6-deoxytalose (23). The
89 overall aim of the current study was to determine if the exopolysaccharide produced by *B.*
90 *longum* **35624** is related with the immunoregulatory effects of this microorganism. To address
91 this aim, we investigated if an isogenic derivative of *B. longum* **35624**, which does not
92 produce exopolysaccharide, is able to exert similar immunological effects to its parent strain
93 *in vitro* and in colitis and asthma mouse models.

94

95 **MATERIALS AND METHODS**

96 **Bacterial strains, plasmids and culture conditions.** Bacterial strains and plasmids used in
97 this study are detailed in Table 1. Bifidobacteria were routinely cultured in either de Man
98 Rogosa and Sharpe medium (MRS; Oxoid Ltd., Basingstoke, Hampshire, United Kingdom)
99 supplemented with 0.05 % cysteine-HCl or reinforced clostridial medium (RCM; Oxoid Ltd.).
100 Bifidobacterial cultures were incubated at 37 °C under anaerobic conditions in a Don Whitley
101 anaerobic Chamber. *Escherichia coli* strains were cultured in Lysogeny broth (LB; Oxoid
102 Ltd) at 37 °C with agitation. Where appropriate, growth media contained chloramphenicol
103 (Cm; 10 µg ml^{-1} for *E. coli* and 5 µg ml^{-1} for *B. longum* **35624**), erythromycin (Em; 100 µg
104 ml^{-1} for *E. coli*), tetracycline (Tet; 10 µg ml^{-1} for *E. coli* and 10 µg ml^{-1} for *B. longum* **35624**),
105 ampicillin (Amp; 100 µg ml^{-1} for *E. coli*) or kanamycin (Km; 50 µg ml^{-1} for *E. coli*). All
106 antibiotics were obtained from Sigma Aldrich, Dorset, England). The commercially available
107 *B. longum* **35624™** culture was provided by Alimentary Health limited (Cork, Ireland).

108 **DNA manipulations.** Chromosomal DNA was isolated from bifidobacteria as
109 previously described (24). Minipreparation of plasmid DNA from *E. coli* or *B. longum* **35624**
110 was achieved using the Qiaprep spin plasmid miniprep kit (Qiagen GmBH, Hilden,
111 Germany). For *B. longum* **35624** an initial lysis step was incorporated into the plasmid
112 isolation procedure, cells were resuspended in lysis buffer supplemented with lysozyme (30
113 mg ml^{-1}) and incubated at 37 °C for 30 min. Restriction enzymes and T4 DNA ligase were
114 used according to the supplier's instructions (Roche Diagnostics, Bell Lane, East Sussex,
115 UK). Synthetic single stranded oligonucleotide primers used in this study were obtained from
116 Eurofins (Ebersberg, Germany) and are detailed in Table 2. Standard PCRs were performed

using TaqPCR mastermix (Qiagen), while high fidelity PCR was achieved using *Pfu*II polymerase (Agilent, Santa Clara, California). *B. longum* **35624** colony PCRs were performed according to standard procedures with the addition of an initial incubation step of 95 °C for 5 minutes to perform cell lysis. PCR fragments were purified using the Qiagen PCR purification kit. Following electroporation of plasmid DNA into *E.coli* strain EC101, electrotransformation of *B. longum* **35624** or sEPS^{neg} was performed essentially as described by Maze *et al*. (25) with the following modifications. An overnight culture of *B. longum* **35624** was sub-cultured twice (first using a 2 % inoculum and then a 1 % inoculum) in MRS supplemented with 0.05 % cysteine-HCl and 0.2 M sucrose prior to inoculating (4%) modified Rogosa medium supplemented with 0.05 % cysteine-HCl, 1% (w/v) glucose and 0.2 M sucrose. Bacteria were grown until the OD_{600} had reached 0.3-0.4, after which cells were harvested by centrifugation (6,500 rpm, 10 min, and 4 °C) and washed twice using 1 mM ammonium citrate buffer (pH 6.0) supplemented with 0.5 M sucrose. An additional centrifugation step (9,800 *g, 10 min, and 4 °C) was included to concentrate the competent cells. For electroporation 5 µl of plasmid DNA was mixed with 50 µl of competent cells, transferred into an electroporation cuvette with 0.2 cm inter-electrode distance and pulsed at 2.5 kV, 25 µF and 200 Ω using a Gene Pulser II Electroporation System (Biorad, Hercules, California USA). For recovery, 800 µl of RCM supplemented with 0.05 % L-cysteine hydrochloride were added to bacteria and incubated anaerobically for 2.5 h at 37 °C. Transformations were plated on reinforced clostridial agar (RCA) plates supplemented with appropriate concentrations of relevant antibiotics and incubated 2-3 days anaerobically at 37 °C. The correct orientation and integrity of all constructs was verified by PCR and subsequent DNA sequencing, which was performed at Eurofins (Ebersberg, Germany).

Construction of sEPS^{neg}. An internal 583 bp fragments of the *pgt*$_{624}$ gene was amplified by PCR using *B. longum* **35624** chromosomal DNA as a template and the oligonucleotide primers *BI0342F_HindIII* and *BI0342R_XbaI*. The PCR product generated was ligated to pORI19, an Ori^{+} RepA- integration plasmid (26), using the unique *HindIII* and *XbaI* restriction sites that were incorporated into the primers for the *pgt* fragment-encompassing amplicon, and introduced into *E. coli* EC101 by electroporation. Recombinant *E. coli* EC101 derivatives containing pORI19 constructs were selected on LB agar containing Em, and supplemented with X-gal (5-bromo-4-chloro-3-indolyl-β-D-galactopyranoside) (40 μg ml^{-1}) and IPTG (isopropyl-β-D galactopyranoside) (1 mM). The expected genetic structure of the recombinant plasmid, designated pORI19-*pgt*, was confirmed by restriction mapping prior to subcloning of the Tet resistance antibiotic cassette, *tet(W)*, from pAM5 (27) as a *SacI* fragment into the unique *SacI* site on pORI19-*pgt*. The expected structure of a single representative of the resulting plasmid, designated pORI19*tet(W)_pgt*, was confirmed by restriction analysis. The plasmid was introduced into *E. coli* EC101 harbouring pNZ-M.1185 (this is a plasmid expressing a *B. longum* **35624**-encoded methylase) by electroporation, and transformants were selected based on Em and Tet resistance. Methylation of the resulting plasmid complement of such transformants by the *M.1185* (isoschizomer of *M.EcoRII*) was confirmed by their observed resistance to *EcoRII* restriction. Plasmid preparations of methylated pORI19*tet(W)_pgt* were introduced by electroporation into *B. longum* **35624** with subsequent selection on RCA plates supplemented with Tet.

Construction of sEPS^{comp}. For the construction of plasmid pBC1.2_*pgt*$_{624}$ +*BI0343*, a DNA fragment encompassing *pgt*$_{624}$ plus the downstream located gene with locus tag BI0343 and the presumed promoter region was generated by PCR amplification from chromosomal

DNA of *B. longum* **35624** using *Pfu*II polymerase and primer combinations BI0342FSalI and BI0343EcoRI, where *SalI* or *EcoRI* restriction sites were incorporated at the 5' ends of the forward primer, and reverse primer, respectively. Amplicons were digested with *Sal*I, and *Eco*RI, and ligated into similarly digested pBC1.2 prior to introduction into *E. coli* XL1blue by electroporation and subsequent selection of transformants on LB agar supplemented with Tet and Amp. The integrity of positive clones was confirmed by sequencing and one selected clone designated pBC1.2 *pgt+BI0343* was introduced into sEPS^{neg} by electroporation with subsequent selection of transformants on RCA supplemented with Tet and Cm. The resultant sEPS^{neg} strain harboring pBC1.2 *pgt+BI0343* was designated sEPS^{comp}.

Electron Microscopy. After culture in MRS medium, bacteria were gently rinsed in Piperazine-N,N-bis-2-ethane sulphonic acid (PIPES) buffer (0.1 M, pH 7.4) before being fixed in 2.5 % glutaraldehyde in PIPES buffer for 5 min. The samples were rinsed twice (2 min each time) in PIPES buffer and post-fixed with 1 % osmium tetroxide in 0.1 M PIPES buffer (pH 6.8), for 60 min in the dark. The samples were rinsed three times in double distilled water (2 min each wash) before dehydration through an ethanol series (50, 70, 96, and 100 %) for 5 min each. All fixation and washing steps were carried out at room temperature. Following dehydration, the samples were critically point dried in a POLARON E3100 critical point drier (Agar Scientific, Stansted, UK), and coated with 10 nm of gold/palladium (80/20) using a Baltec MED 020 unit (Baltec, Buchs, Liechtenstein). Bacterial preparations were examined using a Hitachi S-4700 scanning electron microscope (SEM), operated in secondary electron detection mode (3 kV, 40 µA) and images captured with Quartz PCI (Quartz Imaging Corporation, Vancouver, Canada).

185 **Exopolysaccharide isolation.** The exopolysaccharide was isolated as previously
186 described (23). Briefly, following harvesting of *B. longum* **35624** cells, which were grown on
187 agar plates to minimize carryover of media components, an exopolysaccharide solution was
188 generated by agitating the cells in PBS. The harvested exopolysaccharide solution was mixed
189 with ethanol and the exopolysaccharide aggregated at the center of the surface of the ethanol
190 solution, which facilitated harvesting of the exopolysaccharide without the need for
191 centrifugation. The exopolysaccharide aggregations were taken with a spatula, resuspended in
192 water and dialysed against water to remove contaminants and residual ethanol. The
193 exopolysaccharide was applied 2 times on Bakerbond SPE C18 columns (Avantor, Deventer,
194 The Netherlands) as indicated by the manufacturer using a HyperSep-96™ vacuum manifold
195 (Thermo Scientific, Waltham, USA). The flow-through fraction was collected and filtered
196 through 0.45 µm syringe filters. Quantification of total carbohydrate levels was performed as
197 previously described (28) using a phenol-sulphuric acid method in microplate format. The
198 absence of contaminating proteins was confirmed by measuring the total soluble protein
199 content of the exopolysaccharide preparation using the BCA protein quantification kit
200 (Thermo Scientific) according to manufacturer's instructions. Bovine serum albumin was
201 used for generation of standards. Lipopolysaccharide contamination was monitored using the
202 pyrogene recombinant factor C assay (Lonza, Bettlach, Switzerland).

203 ***In vitro* immune assays.** Human blood was purchased from the Swiss blood bank
204 (Blutspendezentrum, Basel, Switzerland), which obtains the blood following appropriate
205 screening and consenting of volunteers. Blood samples were anonymized and coded prior to
206 leaving the blood bank. Research procedures on human blood were performed in accordance
207 with Swiss law (ethical approval number KEK Nr. 19/08). All experiments with human
208 blood-derived cells were conducted under biosafety level 2 conditions. Peripheral blood

209 mononuclear cells (PBMCs) were isolated from healthy donors using density gradient
210 centrifugation. Human monocyte-derived dendritic cells (MDDCs) were differentiated with
211 1000 IU ml^{-1} GM-CSF (Peprotech, London, UK) and 1000 IU ml^{-1} IL-4 (Novartis, Basel,
212 Switzerland) from purified $CD14^+$ cells using MACS separation (Miltenyi Biotec, Bergisch
213 Gladbach, Germany). Bacterial strains for *in vitro* assays were cultured in MRS medium
214 supplemented with 0.05 % L-cysteine for 48 hours under anaerobic conditions at 37°C. Cells
215 were harvested and washed once with sterile PBS by centrifugation at 6,500 rpm for 10
216 minutes. Bacterial cell number was determined by microscopy using a Petroff-Hausser
217 chamber and bacteria were diluted as appropriate in PBS for incubation with human cells.
218 PBMCs and MDDCs were stimulated for 24 h at 37°C, 5 % CO_2 with bacterial strains at a
219 concentration of 50 bacterial cells to 1 PBMC or MDDC. Human and bacterial cell co-
220 cultures were performed in complete RPMI-1640 (cRPMI) medium (Sigma, Buchs,
221 Switzerland) supplemented with 10% fetal bovine serum (Sigma), penicillin (100 Units ml^{-1})
222 and streptomycin (0.1 mg ml^{-1}) (Sigma). Purified exopolysaccharide from *B. longum* **35624**
223 was also added (final concentration 100 µg/ml) to PBMC cultures (in duplicate) stimulated
224 with $sEPS^{neg}$. Cytokine concentrations were measured using the Bio-Plex Multiplex System
225 (Biorad). For human dendritic cells staining, the following anitibodies were used: PE-Cy7
226 anti-human CD274 (PD-L1), APC anti-human CD273 (PD-L2) and Pacific Blue anti-human
227 CD11c (eBioscience, Vienna, Austria). THP-1-Blue™ NF-κB monocyte cell line (Invivogen,
228 San Diego, USA) was maintained and sub-cultured in cRPMI medium (Sigma) in presence of
229 200µg/ml Zeocin (Invivogen). For the co-culture experiment with bacteria, 10^5 cells/well
230 were seeded in a 96 well-plate in a total volume of 200 µl/well of cRPMI medium. The cells
231 were stimulated over a range of different bacterial concentrations for 24 h and activation of
232 NF-κB/AP-1 pathway was evaluated by Quanti-Blue™assay according to the manufacturer's

233 instructions. In addition, MDDCs were stimulated with different bacterial strains and NF-κB
234 phosphorylation measured over a time course. MDDCs were lysed using Bio-Plex Pro cell
235 signaling reagent kit (Biorad) and cell lysates were stored at -80°C until analysis. Protein
236 concentration was determined using Bio-Rad's DC™ protein assay and equal amounts of
237 protein were used to measure NF-κB p65 (Ser^{536}) in the Bio-Plex Pro™ Magnetic Cell
238 Signaling Assay (Biorad). Results are expressed as MFI (mean fluorescence intensity).

239 **T cell transfer colitis model.** C.B-17 severe combined immunodeficient (SCID and
240 BALB/c female mice (8-12 weeks of age) were obtained from Charles River (Sulzfeld,
241 Germany) and maintained under specific pathogen free conditions. The animals were housed
242 at the AO Research Institute, Davos, Switzerland, in individually ventilated cages for the
243 duration of the study, and all experimental procedures were carried out in accordance with
244 Swiss law (Permit number: 2013_32). Colitogenic $CD4^+CD25^-CD45RB^{hi}$ cells were isolated
245 from BALB/c donor mouse spleens using the MACS Miltenyi system (depletion of
246 CD4+CD25+ cells followed by positive selection of CD45RB FITC-labeled cells). At day 0,
247 colitis was induced by intraperitoneal transfer of 4×10^5 cells per C.B-17 SCID mouse (8
248 mice per group). Bacterial cells were prepared as described above and counted using
249 microscopy (Petroff-Hausser chamber) prior to dilution in sterile PBS. 1×10^9 *B. longum*
250 **35624** cells, or its isogenic derivatives, were administered to each mouse by intragastric
251 gavage (total volume of 200 µl). Bacteria were gavaged from the beginning of the study (day
252 0) and continued to be gavaged every second day until animals were euthanized at the end of
253 the study. Sixteen days after study initiation, disease severity scores were recorded, while
254 animal weights were monitored every day. Disease severity scores included feces condition (
255 1 - wet; 2 - diarrhea; 3 - bloody diarrhea or rectal prolapse), activity (1 - isolated, abnormal

position; 2 - huddled, hypoactive or hyperactive; 3 – unconscious), coordination of movement (1 - slightly uncoordinated; 2 – very uncoordinated; 3 – paralysis) and fur quality (1 – reduced grooming; 2 – disheveled; 3 - hair loss). Gut transit was determined by quantifying fecal *B. longum* **35624** levels by PCR. *B. longum* **35624** specific primers were designed using Primer3 software (http://simgene.com/Primer3). The primers, designated 2420t (Forward: CAG TGG GGT GCG ACT ACA; Reverse: GCG CGA ACC AGA AGA TGT) generated a 494 bp amplicon. Bacterial DNA from fecal samples was extracted using QIAamp DNA Stool Mini Kit (Qiagen). DNA was quantified using Nanodrop (Thermo Scientific) and 100 ng of total DNA was assayed using SYBR Green PCR Master Mix (Biorad). The thermal cycling conditions consisted of an initial denaturation step of 15 min at 95˚C, followed by 30 cycles of denaturation at 94˚C for 45 sec, annealing for 45 sec at 56˚C, and extension at 72˚C for 45 sec. *B. longum* **35624** DNA concentrations were quantified using the absolute quantitation protocol of the ABI 7900 Fast real-Time PCR system (Applied Biosystem, CA, USA). In a parallel experiment, BALB/c healthy mice (6 mice per group) were gavaged with *B. longum* **35624** or its isogenic derivative for 3 weeks, as described above for the colitis study.

Following euthanasia on day 26, mesenteric lymph nodes were isolated in order to obtain single cell suspensions. Lymph nodes were mechanically disrupted using a syringe plunger to grind the nodes on a nylon cell strainer (70 µm). The strainer was washed with PBS and the single cell suspensions were centrifuged at 300 g for 10 minutes. Cell pellets were resuspended in 1 ml of cRPMI medium (Sigma) and cells were counted using a Scepter Cell Counter (Millipore, Billerica, MA, USA). Cells were diluted to a final density of $1x10^6$cells ml^{-1} in cRPMI and cells were dispensed in propylene tubes to perform FACS staining. Lamina propria mononuclear cells were isolated as described previously (29) following removal of epithelial cells and collagenase VIII/DNaseI (Roche) digestion of the

tissue. At the end of the process, cells were counted using the Scepter Cell Counter (Millipore) and diluted to a final concentration of $1x10^6$ cells ml^{-1} in cRPMI in propylene FACS staining tubes.

OVA respiratory allergy model. Female BALB/c mice (8-12 weeks of age) were obtained from Charles River and were maintained under specific pathogen free conditions at the AO Research Institute, Davos, Switzerland, in individually ventilated cages for the duration of the study. All experimental procedures were carried out in accordance with Swiss law (Permit number: 2013_20). 8 mice per group were used in this model. Three intraperitoneal immunizations with 50 µg of ovalbumin (OVA, Grade V>98%, Sigma) emulsified in Imject™ Alum Adjuvant (Life Technologies, Carlsbad, California, USA) were performed on days 0, 14 and 21, followed by OVA aerosol challenges on days 26, 27 and 28. On days 19, 25 and 27, mice received *B. longum* **35624** or $sEPS^{neg}$ intra-nasally (~$1x10^9$ bacteria per dose in a total volume of 50 µl of PBS). Bacterial cells were prepared as described above. Control animals received three intraperitoneal injections with Alum adjuvant (without OVA) on days 0, 14 and 21, followed by OVA aerosol challenges on days 26, 27 and 28. Control animals also received 50 µl of PBS intra-nasally on days 19, 25 and 27. All mice were sacrificed at day 29 for isolation of lung tissue and flow cytometric staining. Lung-derived single cell suspensions were obtained using a combination of enzymatic digestion (lung dissociation kit, Miltenyi) and mechanical dissociation with a gentleMACS Dissociator (Miltenyi), according to the manufacturer's protocol. Lung cells were plated at $1x10^6$ cells/ml in complete RPMI (Sigma) and stimulated *ex vivo* with 50 µg/ml OVA grade VI (Sigma) or with 500 ng/ml LPS (Sigma) for 48 hours and cytokine secretion quantified by the Bio-Plex Multiplex System (Biorad).

303 **Flow cytometry.** All flow cytometry analyses were performed on the Gallios Flow
304 Cytometer (Beckman Coulter, Brea, USA). Mesenteric lymph node or lung single cell
305 suspensions were stimulated with PMA and ionomycin at 50 ng ml^{-1} and 500 ng ml^{-1},
306 respectively, for 4 hours in presence of Brefeldin A (eBioscience). Viability dye eFluor780
307 (eBioscience) and the following surface staining antibodies were used: PE-Cy7 anti-mouse
308 CD3 and Pacific Blue anti-mouse CD4 (Biolegend, San Diego, California USA). Cells were
309 stained for intracellular cytokines using PE anti-mouse IL-10, Alexa Fluor488 anti-mouse/rat
310 IL-17A and PerCP-Cy5.5 anti-mouse IFN-γ after fixation and permeabilization (Intracellular
311 Fixation & Permeabilization Buffer Set, eBioscience). Lamina propria cells were in addition
312 stained for the gut homing molecule CCR9 using Alexa Fluor647 anti-mouse CD199 (CCR9)
313 from Biolegend.

314 **Statistical analysis.** Unless otherwise indicated, data are presented as box-and-
315 whisker plots with the median value and max/min values illustrated. In experiments with
316 technical replicates, the mean was calculated from the technical replicates for each donor and
317 only the mean value was used for the statistical analysis. The Mann–Whitney U test was used
318 for the nonparametric statistical analysis of differences between two groups. For analysis of
319 more than two groups, statistical significance was determined using the Kruskal–Wallis test
320 and Dunn's multiple comparison test. A two-way ANOVA was used to compare groups over
321 time. A p-value less than 0.05 was considered statistically significant.

322

323 **RESULTS**

324 **Generation of an isogenic exopolysaccharide-negative derivative of *B. longum* 35624,**
325 **designated sEPS^{neg}, by insertion mutagenesis.** In order to determine the role, if any, of the

326 exopolysaccharide in the reported immunomodulatory activities of the *B. longum* **35624**
327 strain, we set out to generate an isogenic derivative of this strain that was unable to produce
328 this cell surface-associated glycan exopolymer. For this purpose, we employed a mutagenesis
329 strategy that was based on previously described methods (30). The particular mutagenesis
330 strategy employed for *B. longum* **35624** involved the heterologous expression of a *B. longum*
331 **35624**-encoded DNA methylase in *E. coli* strain EC101 so as to methylate any plasmid DNA
332 in this latter cloning host. When such methylated plasmid DNA is subsequently introduced
333 into *B. longum* **35624**, it will be protected from digestion by the native restriction-
334 modification systems encoded by the latter strain and will therefore allow homology-guided,
335 site-directed mutagenesis as has been described previously (30). Employing this strategy, we
336 created an insertion mutation in the first gene of the eps_{624} cluster, i.e. pgt_{624}, encoding the
337 predicted priming glycosyl transferase (pGT), resulting in an isogenic derivative of *B. longum*
338 **35624**, which was designated $sEPS^{neg}$.

339 In order to assess if the $sEPS^{neg}$ mutant had, as would be expected, lost its ability to
340 produce exopolysaccharide we performed electron microscopy analysis, which indeed
341 revealed that the 'stringy' sEPS layer present on the parent strain *B. longum* **35624** is absent
342 on EPS^{neg}, thus confirming its exopolysaccharide-deficient phenotype (Fig. 1). Furthermore,
343 and in contrast to the parent strain *B. longum* **35624**, the EPS^{neg} strain exhibits a so-called
344 dropping phenotype when grown in liquid medium (i.e. the EPS^{neg} strain was found to
345 sediment during growth in liquid medium, but the *B. longum* **35624** strain remained in
346 suspension). A similar phenotype was observed for exopolysaccharide-negative variants of *B.*
347 *breve* UCC2003 and *Bifidobacterium animalis* subs. *lactis* (21, 31), thereby substantiating the
348 loss of exopolysaccharide production. To ensure that the observed phenotype is directly
349 linked to the inactivation of pgt_{624}, the adjacent and co-transcribed genes pgt_{624} and *BI0343*

were cloned together with the presumed promoter sequence in plasmid pBC1.2, after which the resultant construct was introduced in the sEPS^{neg} strain. The resulting strain, designated sEPS^{comp}, was shown to produce exopolysaccharide (Fig. 1). A similar complementation approach was previously described (32, 33). The sEPS^{neg} and sEPS^{comp} mutants grew more slowly compared to the parent strain *B. longum* **35624**, likely due to the presence of antibiotics in their culture media, but by 38 hours of culture all bacteria were at similar numbers and had reached stationary phase (Supplementary Fig. S1).

***In vitro* responses to *B. longum* 35624, sEPS^{neg} and sEPS^{comp}.** The wild-type strain *B. longum* **35624** and its derivatives sEPS^{neg} or sEPS^{comp} were co-incubated with human PBMCs for 24 hours, followed by analysis of cytokine secretion in cell-free supernatants. As compared with *B. longum* **35624,** the sEPS^{neg} strain was shown to induce higher levels of IL-12p70, IFN-γ and IL-17 secretion, with comparable induction of IL-10 (Fig. 2A). The sEPS^{comp} strain induced similar levels of cytokine secretion as *B. longum* **35624**, confirming that enhanced pro-inflammatory cytokine secretion is specifically associated with the lack of exopolysaccharide production. The addition of isolated exopolysaccharide to the co-cultures significantly reduced IL-12p70 and IFN-γ secretion in response to the sEPS^{neg} strain, but did not alter IL-17 or IL-10 responses to the sEPS^{neg} strain (Fig. 2B).

Similarly to PBMCs, human MDDCs were co-incubated with *B. longum* **35624** or sEPS^{neg} strains, and cytokine secretion was measured after a 24 hour exposure. Secreted IL-17, IL-6 and TNF-α levels, but not IL-10, were all shown to be significantly higher for the sEPS^{neg}-stimulated MDDCs, compared to *B. longum* **35624** -stimulated MDDCs (Fig. 3A). In contrast, no differences were found in the *B. longum* **35624** or sEPS^{neg} –induced expression of the MDDC inhibitory molecules programmed death-ligand 1 (PD-L1) and PD-L2, which bind

373 to PD-1 on activated lymphocytes and play an important role in down-regulating the immune
374 system (Fig. 3B).

375 Activation of the transcription factor NF-κB is critical for the induction of
376 inflammatory genes, including cytokines. Thus, we measured NF-κB activation in the
377 monocyte cell line THP-1, containing a SEAP reporter for NF-κB and AP-1 activation. The
378 sEPS^{neg} strain was shown to induce higher levels of NF-κB/AP-1 activation, compared to *B.*
379 *longum* **35624**-stimulated THP-1 cells (Fig. 3C). To confirm this result, NF-κB
380 phosphorylation was measured in MDDCs over time, following exposure to bacteria. Both *B.*
381 *longum* **35624** and sEPS^{neg} strains induced similar levels of NF-κB phosphorylation at early
382 time points (Fig. 3D). However, sustained high levels of phosphorylated NF-κB were
383 observed at later time points for the sEPS^{neg}-stimulated MDDCs, which were not observed for
384 *B. longum* **35624**-stimulated cells.

385 Taken together, these results suggest a role for this exopolysacharide in preventing *in*
386 *vitro* inflammatory responses to *B. longum* **35624**.

387 **The sEPS^{neg} strain does not protect against colitis development.** Colitis was
388 induced in SCID mice by adoptively transferring CD4^{+}CD25^{-}CD45RB^{hi} lymphocytes. Mice
389 were administered *B. longum* **35624**, sEPS^{neg} or sEPS^{comp} daily by oral gavage. As previously
390 described, *B. longum* **35624** treatment prevented weight loss and disease symptoms in this
391 model (34). However, mice treated with the sEPS^{neg} strain exhibited significant weight loss
392 and severe disease symptoms, while restoration of EPS production in the sEPS^{comp} strain
393 promoted a similar response as to *B. longum* **35624** (Fig. 4A). Following euthanasia, the
394 colon:body weight ratio was significantly higher in animals administered the sEPS^{neg} strain,

while macroscopically the colons of these mice appeared severely inflamed with visible necrotic regions, which was not observed when animals had been administered *B. longum* **35624** (Fig. 4B). Within the mesenteric lymph nodes, there were significantly more IL-17$^+$ lymphocytes in animals administered the sEPS^{neg}, with a trend towards increased numbers of IFN-γ^+ lymphocytes, which was not statistically significant (Fig. 4C). No significant difference in IL-10$^+$ lymphocytes was observed. No differences in the gastrointestinal transit of *B. longum* **35624** or the sEPS^{neg} derivative was observed (Supplementary Fig. S2).

The administration of the sEPS^{neg} strain to healthy immunocompetent animals did not result in gastrointestinal inflammation, indicating that the sEPS^{neg} mutant did not induce colitis in healthy animals. However, administration of sEPS^{neg} did provoke a trend in an increased percentage of IL-17$^+$ and IFN-γ^+ lymphocytes, associated with an increase in CCR9$^+$ T cells, within the lamina propria of healthy animals, although these differences did not reach statistical significance (Supplementary Fig. S3). These data suggest that an inflamed micro-environment, such as that present in the SCID model, is required for sEPS^{neg} to exert its T_H17-enhancing effects.

sEPS^{neg} exacerbates IL-17 responses within the lung. In order to further assess the ability of sEPS^{neg} to promote IL-17 responses *in vivo*, we utilized the ovalbumin (OVA) sensitization and respiratory challenge model, as we and others previously evidenced potent T_H17 responses within the lungs of challenged animals (35). Either the *B. longum* **35624** or its isogenic derivative sEPS^{neg} were administered intra-nasally to examine the influence of these strains on IL-17 responses within the lung. OVA sensitization and challenge resulted in an increased percentage of IL-17$^+$ lymphocytes within lung tissue, compared to control animals (Fig. 5A). Exposure to the *B. longum* **35624** strain did not influence the percentage of IL-17$^+$

418 lymphocytes within the lung, however, exposure to sEPS^{neg} significantly increased the
419 percentage of IL-17^{+} lymphocytes (Fig. 5A). Single cell suspensions were generated from the
420 lungs of all animals challenged as indicated above, and these lung cells were re-stimulated *ex*
421 *vivo* with OVA or LPS to assess IL-17 secretion. OVA sensitized and challenged animals
422 displayed increased *ex vivo* secretion of IL-17 to both OVA and LPS stimulation, compared to
423 non-sensitized animals, suggesting that innate TLR-4 responses to LPS and allergen-specific
424 lymphocyte responses to OVA are increased in the inflamed lungs of allergic animals (Fig.
425 5A). The *in vivo* exposure to *B. longum* **35624** did not alter the *ex vivo* secretion of IL-17 by
426 lung cells stimulated with either LPS or OVA. However, if animals had been exposed to
427 sEPS^{neg} *in vivo* previously, the isolated lung cells secreted significantly more IL-17 *ex vivo* in
428 response to both TLR-4 stimulation with LPS and allergen restimulation with OVA (Fig. 5A).
429 Thus, *ex vivo* secretion of IL-17 and the percentage of IL-17^{+} cells within lung tissue correlate
430 with the highest levels for both assay systems being observed for sEPS^{neg}-treated animals.

431 OVA sensitization and challenge resulted in an increased percentage of IFN-γ^{+}
432 lymphocytes within lung tissue, compared to control animals (Fig. 5A). Exposure to the *B.*
433 *longum* **35624** strain prevented the increase in the percentage of IFN-γ^{+} lymphocytes within
434 the lung, which was not observed following exposure to the sEPS^{neg} strain (Fig. 5B). Re-
435 stimulation of lung single cell suspensions *ex vivo* with OVA or LPS did not result in
436 significant levels of IFN-γ being secreted and no statistically significant differences were
437 observed between the groups (Fig. 5B).

438 OVA sensitization and challenge resulted in an increased percentage of IL-10^{+}
439 lymphocytes within lung tissue and exposure to *B. longum* **35624** or the sEPS^{neg} strains
440 further increased the percentage of IL-10^{+} lymphocytes within the lung (Fig. 5C). Re-

441 stimulation *ex vivo* was also associated with increased secretion of IL-10 following *in vivo*
442 exposure to *B. longum* **35624** or the sEPS^{neg} strains (Fig. 5C).

443 These findings suggest that the absence of the exopolysaccharide on *B. longum* **35624**
444 promotes T_H17 responses in the inflamed lung, similar to the effects described above for the
445 inflamed gut.

446

447 **DISCUSSION**

448 In order to avoid immune-mediated destruction of mucosal tissues, the host can activate
449 regulatory mechanisms that can block proinflammatory responses to commensal microbes
450 present on mucosal surfaces. Bifidobacteria comprise a significant proportion of the gut
451 microbiota and many strains are currently used as probiotics. However, the precise
452 mechanisms by which such bifidobacteria interact with host immune cells are not fully
453 understood. In this report we describe that the presence of a cell surface-associated
454 exopolysaccharide produced by *B. longum* **35624** modulates cytokine secretion and NF-κB
455 activation *in vitro*, while in murine models exposure to a *B. longum* **35624** derivative unable
456 to synthesize exopolysaccharide promotes T_H17 responses both within the gut and the lung.

457 Bifidobacterial cell surface-associated exopolysaccharides have previously been
458 proposed to (i) mediate some of their health-promoting benefits, (ii) contribute to their
459 tolerance of the harsh conditions within the gut, and (iii) to influence composition of the gut
460 microbiome through their use as a fermentable substrate by other microbes (36-39). In
461 general, bacterial exopolysaccharide consists of repeating mono- or oligosaccharide subunits
462 connected by varying glycosidic linkages, which are structurally very diverse, and which may

463 contribute to strain-specific traits due to the expected structural and therefore functional
464 diversity of such molecules. Of note, pathogen-associated exopolysaccharides have long been
465 known to be critical in host–microbe interactions, where they facilitate adherence and
466 colonization within the human host, with additional immunomodulatory effects (40, 41).
467 Exopolysaccharides can also mediate the beneficial immune effects associated with certain
468 commensal microbes. As already mentioned, a strong modulator of intestinal immune
469 responses is PSA from *B. fragilis*, which is well described to influence lymphocyte
470 polarization and PSA suppresses IL-17 production by intestinal immune cells (42-44). In line
471 with data presented in this manuscript, exopolysaccharide gene knockout mutants of
472 *Lactobacillus casei* Shirota induced significantly more pro-inflammatory cytokine secretion
473 from a mouse macrophage cell line, compared to wild-type cells (45). In addition, the
474 cytokine response of PBMCs to two isogenic strains of *B. animalis* subsp. *lactis* that differ
475 only in their exopolysaccharide-producing phenotype suggest that the mucoid strain could
476 have higher anti-inflammatory activity (31). The data presented in this manuscript are in
477 agreement with these previous reports and further supports the concept that
478 exopolysaccharides from bifidobacteria may elicit immune-modulatory activities.

479 Interestingly, the induction of PD-L1 and PD-L2 on dendritic cells was similar for the
480 wild type *B. longum* **35624** strain and its isogenic derivative sEPS^{neg}. Similarly, the induction
481 of IL-10 was not negatively impacted by the loss of exopolysaccharide from the bacterium.
482 This suggests that not all immune-regulatory effects induced by *B. longum* **35624** are
483 mediated solely by exopolysaccharide. The bifidobacterial cell wall is a complex arrangement
484 of macromolecules, consisting of a thick peptidoglycan layer that surrounds the cytoplasmic
485 membrane, which is decorated with other glycopolymers, such as (lipo)teichoic acids,
486 polysaccharides and proteins, all of which may influence the immune response (46, 47) A few

examples include the cell wall-associated proteins p40 and p75 from *L. casei* ssp. *rhamnosus* GG, the S-layer protein from *L. acidophilus*, or the STp peptide from *L. plantarum* (48-50) .

T_H17 cells are a subset of CD4+ T helper cells that mediate protective immunity to extracellular bacterial and fungal pathogens, predominantly at epithelial surfaces (51). Polarization of naïve T cells into T_H17 cells occurs following T-cell antigen receptor recognition of an MHC class II-bound peptide in the presence of cytokines including TGF-β1, IL-6 or IL-1β (52, 53). While T_H17 cells are required for protective immunity, these cells massively infiltrate the inflamed intestine of inflammatory bowel disease patients, where they produce IL-17 and other cytokines, triggering and amplifying the inflammatory process (54). Our data suggests that the *B. longum* **35624** strain-associated exopolysaccharide prevents the induction of a T_H17 response to this bacterium. Multiple mechanisms may be involved in this process. For example the exaggerated induction of cytokines, including IL-6, from dendritic cells may support T_H17 lymphocyte polarization and development. Support for this hypothesis can be seen when we restimulate OVA-specific T cells with OVA and we observe increased secretion of IL-17 when the lungs were previously exposed to $sEPS^{neg}$. These OVA-specific T cells are not reacting to bifidobacteria-associated antigens, but more IL-17 is secreted upon OVA challenge suggesting that it is the cytokine microenvironment, provided by innate cells such as dendritic cells, that is supporting excessive T_H17 development. The observation that addition of purified exopolysaccharide to $sEPS^{neg}$-stimulated PBMCs suppresses the exaggerated IL-12p70 and IFN-γ secretion, but not IL-17 secretion, also suggests that multiple mechanisms may be involved. Future studies will determine if it is the exopolysaccharide itself that can directly inhibit T_H17 responses by binding to host receptors,

or if the exopolysaccharide is simply masking T_H17-promoting molecules on the surface of this bacterium.

In conclusion, we have identified a novel immunoregulatory activity associated with the presence of a exopolysaccharide in the human commensal *B. longum* **35624** strain. Our findings suggest that this exopolysaccharide is required to prevent a potent tissue-damaging T_H17 response to a commensal bacterium. Accordingly, our data on the *B. longum* 35624-associated exopolysaccharide corroborates, and expands, the published concept that exopolysaccharides produced by certain lactic acid bacteria and bifidobacteria may elicit immune-modulatory activities (55), which are important for appropriate host-microbe communication.

Funding information. These studies were directly supported by a European Union Marie Curie training network, entitled "TEAM-EPIC". In addition, the authors are supported by Swiss National Foundation grants (project numbers CRSII3_154488 and 310030_144219), Christine Kühne Center for Allergy Research and Education, and by Science Foundation Ireland (SFI) (Grant No. SFI/12/RC/2273). Mary O'Connell Motherway is a recipient of a HRB postdoctoral fellowship (Grant No. PDTM/20011/9). Elisa Schiavi was supported by an EAACI Research Fellowship Award 2012.

The funders had no role in study design, data collection and interpretation, or the decision to submit the work for publication.

Acknowledgments. 35624 is a trademark of Alimentary Health Ltd, Cork, Ireland. We thank Patrycja Konieczna for her technical assistance.

REFERENCES

1. **Donaldson GP, Lee SM, Mazmanian SK.** 2016. Gut biogeography of the bacterial microbiota. Nat Rev Microbiol **14:**20-32.
2. **Marchesi JR, Adams DH, Fava F, Hermes GDA, Hirschfield GM, Hold G, Quraishi MN, Kinross J, Smidt H, Tuohy KM, Thomas LV, Zoetendal EG, Hart A.** 2016. The gut microbiota and host health: a new clinical frontier. Gut **65:**330-339.
3. **Frei R, Lauener RP, Crameri R, O'Mahony L.** 2012. Microbiota and dietary interactions - an update to the hygiene hypothesis? Allergy **67:**451-461.
4. **Trompette A, Gollwitzer ES, Yadava K, Sichelstiel AK, Sprenger N, Ngom-Bru C, Blanchard C, Junt T, Nicod LP, Harris NL, Marsland BJ.** 2014. Gut microbiota metabolism of dietary fiber influences allergic airway disease and hematopoiesis. Nat Med **20:**159-166.
5. **Frei R, Akdis M, O'Mahony L.** 2015. Prebiotics, probiotics, synbiotics, and the immune system: experimental data and clinical evidence. Curr Opin Gastroenterol **31:**153-158.
6. **Tomkovich S, Jobin C.** 2016. Microbiota and host immune responses: a love-hate relationship. Immunology **147:**1-10.
7. **Konieczna P, Akdis CA, Quigley EMM, Shanahan F, O'Mahony L.** 2012. Portrait of an immunoregulatory Bifidobacterium. Gut Microbes **3:**261-266.
8. **O'Mahony C, Scully P, O'Mahony D, Murphy S, O'Brien F, Lyons A, Sherlock G, MacSharry J, Kiely B, Shanahan F, O'Mahony L.** 2008. Commensal-Induced Regulatory T Cells Mediate Protection against Pathogen-Stimulated NF-κB Activation. PLoS Pathogens **4:**e1000112.
9. **Lyons A, O'Mahony D, O'Brien F, MacSharry J, Sheil B, Ceddia M, Russell WM, Forsythe P, Bienenstock J, Kiely B, Shanahan F, O'Mahony L.** 2010. Bacterial strain-specific induction of Foxp3 + T regulatory cells is protective in murine allergy models. Clin Exp Allergy **40**:811-9.
10. **McCarthy J, O'Mahony L, O'Callaghan L, Sheil B, Vaughan EE, Fitzsimons N, Fitzgibbon J, O'Sullivan GC, Kiely B, Collins JK, Shanahan F..** 2003. Double blind, placebo controlled trial of two probiotic strains in interleukin 10 knockout mice and mechanistic link with cytokine balance. Gut **52:**975-980.
11. **Scully P, MacSharry J, O'Mahony D, Lyons A, O'Brien F, Murphy S, Shanahan F, O'Mahony L.** 2013. *Bifidobacterium infantis* suppression of Peyer's patch MIP-1α and MIP-1β secretion during *Salmonella* infection correlates with increased local CD4+CD25+ T cell numbers. Cell Immunol **281:**134-140.
12. **Symonds EL, O'Mahony C, Lapthorne S, O'Mahony D, Sharry JM, O'Mahony L, Shanahan F.** 2012. B*ifidobacterium Infantis* 35624 Protects Against Salmonella-Induced Reductions in Digestive Enzyme Activity in Mice by Attenuation of the Host Inflammatory Response. Clin Transl Gastroenterol **3:**e15.
13. **Konieczna P, Groeger D, Ziegler M, Frei R, Ferstl R, Shanahan F, Quigley EMM, Kiely B, Akdis CA, O'Mahony L.** 2012. *Bifidobacterium infantis* 35624 administration induces Foxp3 T regulatory cells in human peripheral blood: potential role for myeloid and plasmacytoid dendritic cells. Gut **61:**354-366.

14. **Groeger D, O'Mahony L, Murphy EF, Bourke JF, Dinan TG, Kiely B, Shanahan F, Quigley EMM.** 2013. *Bifidobacterium infantis* 35624 modulates host inflammatory processes beyond the gut. Gut Microbes **4:**325-339.
15. **Konieczna P, Ferstl R, Ziegler M, Frei R, Nehrbass D, Lauener RP, Akdis CA, O'Mahony L.** 2013. Immunomodulation by *Bifidobacterium infantis* 35624 in the Murine Lamina Propria Requires Retinoic Acid-Dependent and Independent Mechanisms. PLoS One **8:**e62617.
16. **Sibartie S, O'Hara AM, Ryan J, Fanning A, O'Mahony J, O'Neill S, Sheil B, O'Mahony L, Shanahan F**. 2009. Modulation of pathogen-induced CCL20 secretion from HT-29 human intestinal epithelial cells by commensal bacteria. BMC Immunol **10**:54.
17. **O'Mahony L, O'Callaghan L, McCarthy J, Shilling D, Scully P, Sibartie S, Kavanagh E, Kirwan WO, Redmond HP, Collins JK, Shanahan F.** 2006. Differential cytokine response from dendritic cells to commensal and pathogenic bacteria in different lymphoid compartments in humans. Am J Physiol Gastrointest Liver Physiol **290**:839-845.
18. **Round JL, Mazmanian SK.** 2010. Inducible Foxp3+ regulatory T-cell development by a commensal bacterium of the intestinal microbiota. Proc Natl Acad Sci U S A **107:**12204-12209.
19. **Dasgupta S, Erturk-Hasdemir D, Ochoa-Reparaz J, Reinecker HC, Kasper DL.** 2014. Plasmacytoid dendritic cells mediate anti-inflammatory responses to a gut commensal molecule via both innate and adaptive mechanisms. Cell Host Microbe **15:**413-423.
20. **Jones SE, Paynich ML, Kearns DB, Knight KL.** 2014. Protection from intestinal inflammation by bacterial exopolysaccharides. J Immunol **192:**4813-4820.
21. **Fanning S, Hall LJ, Cronin M, Zomer A, MacSharry J, Goulding D, Motherway MO, Shanahan F, Nally K, Dougan G, van Sinderen D.** 2012. Bifidobacterial surface-exopolysaccharide facilitates commensal-host interaction through immune modulation and pathogen protection. Proc Natl Acad Sci U S A **109:**2108-2113.
22. **Rossi O, Khan MT, Schwarzer M, Hudcovic T, Srutkova D, Duncan SH, Stolte EH, Kozakova H, Flint HJ, Samsom JN, Harmsen HJ, Wells JM.** 2015. *Faecalibacterium prausnitzii* Strain HTF-F and Its Extracellular Polymeric Matrix Attenuate Clinical Parameters in DSS-Induced Colitis. PLoS One **10:**e0123013.
23. **Altmann F AF, Kosma P, O'Callaghan A, Leahy S, Bottacini F, Molloy E, Plattner S, Schiavi E, Gleinser M, Groeger D, Grant R, Rodriguez Perez N, Healy S, Svehla E, Windwarder M, Hofinger A, O'Connell Motherway M, Akdis CA, Xu J, Roper J, van Sinderen D, O'Mahony L.** 2016. Genome Analysis and Characterisation of the Exopolysaccharide Produced by *Bifidobacterium longum* subsp. *longum* 35624. PLoS ONE **11**: e0162983.
24. **O'Riordan, Fitzgerald.** 1998. Evaluation of bifidobacteria for the production of antimicrobial compounds and assessment of performance in cottage cheese at refrigeration temperature. J Appl Microbiol **85:**103-114.
25. **Maze A, O'Connell-Motherway M, Fitzgerald GF, Deutscher J, van Sinderen D.** 2006. Identification and Characterization of a Fructose Phosphotransferase System in *Bifidobacterium breve* UCC2003. Appl Environ Microbiol **73:**545-553.
26. **Law J, Buist G, Haandrikman A, Kok J, Venema G, Leenhouts K.** 1995. A system to generate chromosomal mutations in *Lactococcus lactis* which allows fast analysis of targeted genes. J Bacteriol **177:**7011-7018.
27. **Alvarez-Martín P, O'Connell-Motherway M, van Sinderen D, Mayo B.** 2007. Functional analysis of the pBC1 replicon from *Bifidobacterium catenulatum* L48. Appl Microbiol Biotechnol **76:**1395-1402.
28. **Masuko T, Minami A, Iwasaki N, Majima T, Nishimura SI, Lee YC.** 2005. Carbohydrate analysis by a phenol–sulphuric acid method in microplate format. Analytical Biochemistry **339**:69-72.

29. **Arnold IC, Hutchings C, Kondova I, Hey A, Powrie F, Beverley P, Tchilian E.** 2015. *Helicobacter hepaticus* infection in BALB/c mice abolishes subunit-vaccine-induced protection against *M. tuberculosis*. Vaccine **33:**1808-1814.

30. **O'Connell Motherway M, O'Driscoll J, Fitzgerald GF, Van Sinderen D.** 2009. Overcoming the restriction barrier to plasmid transformation and targeted mutagenesis in *Bifidobacterium breve* UCC2003. Microb Biotechnol **2:**321-332.

31. **Hidalgo-Cantabrana C, Sanchez B, Alvarez-Martin P, Lopez P, Martinez-Alvarez N, Delley M, Marti M, Varela E, Suarez A, Antolin M, Guarner F, Berger B, Ruas-Madiedo P, Margolles A.** 2015. A single mutation in the gene responsible for the mucoid phenotype of *Bifidobacterium animalis* subsp. *lactis* confers surface and functional characteristics. Appl Environ Microbiol **81:**7960-7968.

32. **Egan M, O'Connell Motherway M, Ventura M, van Sinderen D.** 2014. Metabolism of sialic acid by *Bifidobacterium breve* UCC2003. Appl Environ Microbiol **80:**4414-4426.

33. **O'Connell Motherway M, Kinsella M, Fitzgerald GF, van Sinderen D.** 2013. Transcriptional and functional characterization of genetic elements involved in galacto-oligosaccharide utilization by *Bifidobacterium breve* UCC2003. Microb Biotechnol **6:**67-79.

34. **van der Kleij H, O'Mahony C, Shanahan F, O'Mahony L, Bienenstock J.** 2008. Protective effects of *Lactobacillus reuteri* and *Bifidobacterium infantis* in murine models for colitis do not involve the vagus nerve. Am J Physiol Regul Integr Comp Physiol **295:**R1131-R1137.

35. **Lu S, Li H, Gao R, Gao X, Xu F, Wang Q, Lu G, Xia D, Zhou J.** 2016. IL-17A, But Not IL-17F, Is Indispensable for Airway Vascular Remodeling Induced by Exaggerated Th17 Cell Responses in Prolonged Ovalbumin-Challenged Mice. J Mol Med (Berl) **194:**3557-3566.

36. **Fanning S, Hall LJ, Cronin M, Zomer A, MacSharry J, Goulding D, O'Connell Motherway M, Shanahan F, Nally K, Dougan G, van Sinderen D.** 2012. Bifidobacterial surface-exopolysaccharide facilitates commensal-host interaction through immune modulation and pathogen protection. Proc Natl Acad Sci U S A **109:**2108-2113.

37. **Salazar N, Ruas-Madiedo P, Kolida S, Collins M, Rastall R, Gibson G, de los Reyes-Gavilán CG.** 2009. Exopolysaccharides produced by *Bifidobacterium longum* IPLA E44 and *Bifidobacterium animalis* subsp. *lactis* IPLA R1 modify the composition and metabolic activity of human faecal microbiota in pH-controlled batch cultures. Int J Food Microbiol **135:**260-267.

38. **Alp G, Aslim B.** 2010. Relationship between the resistance to bile salts and low pH with exopolysaccharide (EPS) production of *Bifidobacterium* spp. isolated from infants feces and breast milk. Anaerobe **16:**101-105.

39. **Salazar N, Gueimonde M, de los Reyes-Gavilán CG, Ruas-Madiedo P.** 2016. Exopolysaccharides Produced by Lactic Acid Bacteria and Bifidobacteria as Fermentable Substrates by the Intestinal Microbiota. Crit Rev Food Sci Nutr **56:**1440-1453.

40. **Conover MS, Sloan GP, Love CF, Sukumar N, Deora R.** 2010. The Bps polysaccharide of *Bordetella pertussis* promotes colonization and biofilm formation in the nose by functioning as an adhesin. Mol Microbiol **77:**1439-1455.

41. **Xu CL, Wang YZ, Jin ML, Yang XQ.** 2009. Preparation, characterization and immunomodulatory activity of selenium-enriched exopolysaccharide produced by bacterium *Enterobacter cloacae* Z0206. Bioresour Technol **100:**2095-2097.

42. **Round JL, Lee SM, Li J, Tran G, Jabri B, Chatila TA, Mazmanian SK.** 2011. The Toll-like receptor 2 pathway establishes colonization by a commensal of the human microbiota. Science **332:**974-977.

43. **Mazmanian SK, Liu CH, Tzianabos AO, Kasper DL.** 2005. An immunomodulatory molecule of symbiotic bacteria directs maturation of the host immune system. Cell **122:**107-118.

44. **Mazmanian SK, Round JL, Kasper DL.** 2008. A microbial symbiosis factor prevents intestinal inflammatory disease. Nature **453:**620-625.
45. **Yasuda E, Serata M, Sako T.** 2008. Suppressive effect on activation of macrophages by *Lactobacillus casei* strain Shirota genes determining the synthesis of cell wall-associated polysaccharides. Appl Environ Microbiol **74:**4746-4755.
46. **Chapot-Chartier M-P, Kulakauskas S.** 2014. Cell wall structure and function in lactic acid bacteria. Microb Cell Fact **13:**S9.
47. **Ruiz L, Hevia A, Bernardo D, Margolles A, Sánchez B.** 2014. Extracellular molecular effectors mediating probiotic attributes. FEMS Microbiol Lett **359:**1-11.
48. **Konstantinov SR, Smidt H, de Vos WM, Bruijns SCM, Singh SK, Valence F, Molle D, Lortal S, Altermann E, Klaenhammer TR, van Kooyk Y.** 2008. S layer protein A of *Lactobacillus acidophilus* NCFM regulates immature dendritic cell and T cell functions. Proc Natl Acad Sci U S A **105:**19474-19479.
49. **Al-Hassi HO, Mann ER, Sanchez B, English NR, Peake STC, Landy J, Man R, Urdaci M, Hart AL, Fernandez-Salazar L, Lee GH, Garrote JA, Arranz E, Margolles A, Stagg AJ, Knight SC, Bernardo D.** 2013. Altered human gut dendritic cell properties in ulcerative colitis are reversed by *Lactobacillus plantarum* extracellular encrypted peptide STp. Mol Nutr Food Res **58:**1132-1143.
50. **Yan F, Cao H, Cover TL, Washington MK, Shi Y, Liu L, Chaturvedi R, Peek RM, Wilson KT, Polk DB.** 2011. Colon-specific delivery of a probiotic-derived soluble protein ameliorates intestinal inflammation in mice through an EGFR-dependent mechanism. J Clin Invest **121:**2242-2253.
51. **Korn T, Bettelli E, Oukka M, Kuchroo VK.** 2009. IL-17 and Th17 Cells. Annu Rev Immunol **27:**485-517.
52. **Veldhoen M, Hocking RJ, Atkins CJ, Locksley RM, Stockinger B.** 2006. TGFβ in the Context of an Inflammatory Cytokine Milieu Supports De Novo Differentiation of IL-17-Producing T Cells. Immunity **24:**179-189.
53. **Akdis M, Burgler S, Crameri R, Eiwegger T, Fujita H, Gomez E, Klunker S, Meyer N, O'Mahony L, Palomares O, Rhyner C, Ouaked N, Schaffartzik A, Van De Veen W, Zeller S, Zimmermann M, Akdis CA.** 2011. Interleukins, from 1 to 37, and interferon-γ: receptors, functions, and roles in diseases. J Allergy Clin Immunol **127**:701-721.
54. **Gálvez J.** 2014. Role of Th17 Cells in the Pathogenesis of Human IBD. ISRN Inflammation **2014:**1-14.
55. **Hidalgo-Cantabrana C, Lopez P, Gueimonde M, de Los Reyes-Gavilan CG, Suarez A, Margolles A, Ruas-Madiedo P.** 2012. Immune Modulation Capability of Exopolysaccharides Synthesised by Lactic Acid Bacteria and Bifidobacteria. Probiotics Antimicrob Proteins **4:**227-237.
56. **Margolles A, Florez AB, Moreno JA, van Sinderen D, de los Reyes-Gavilan CG.** 2006. Two membrane proteins from *Bifidobacterium breve* UCC2003 constitute an ABC-type multidrug transporter. Microbiology **152:**3497-3505.

712 **FIGURE LEGENDS**

713 **Figure 1.** *B. longum* **35624** electron microscopy

714 Representative scanning electron microscopy (SEM) images for the *B. longum* **35624** parent
715 strain (A, upper panel) and its isogenic derivatives, sEPS^{neg} mutant (B, middle panel) and
716 sEPS^{comp} mutant (C, bottom panel) are illustrated. Arrows indicate the 'stringy' layer of
717 extracellular polysaccharide visible on the *B. longum* **35624** parent strain and sEPS^{comp} strain .
718 Scale bars are indicated at the bottom right of each panel.

719

720 **Figure 2.** PBMC cytokine response to bacterial strains

721 (A) PBMCs from 6 healthy donors were stimulated with *B. longum* **35624** or its isogenic
722 derivatives sEPS^{neg} or sEPS^{comp} (50 bacteria:1 PBMC) for 24 hours and cytokine secretion
723 into the culture supernatant was quantified. Data are presented as box-and-whisker plots with
724 the median value and max/min values illustrated. Statistical significance was determined
725 using the Kruskal–Wallis test and Dunn's multiple comparison test (*$p<0.05$). (B) Effect of
726 adding isolated exopolysaccharide on sEPS^{neg} strain-induced PBMC secretion of IL-12p70,
727 IFN-gamma, IL-17 and IL-10. Each line connects the data from the same donor. The Mann–
728 Whitney U test was used for the statistical analysis (*$p<0.05$ versus the sEPS^{neg} strain alone).

729

730 **Figure 3.** MDDC response to bacterial strains

731 MDDCs were generated from 4 healthy donors and were stimulated with *B. longum* **35624** or
732 its isogenic derivative sEPS^{neg} (50 bacteria:1 MDDC) for 24 hours. Cytokine secretion into

the culture supernatant (A) and cell surface expression of the inhibitory molecules PD-L1 or PD-L2 (B) were quantified. Data are presented as box-and-whisker plots with the median value and max/min values illustrated. The Mann–Whitney U test was used for the statistical analysis (*p<0.05 *B. longum* **35624** versus the sEPS^{neg} strain). (C) THP-1 NF-κB activation following exposure to increasing concentrations of *B. longum* **35624** or its isogenic derivative sEPS^{neg} (n=4 experimental replicates). (D) Activation of NF-κB in MDDCs exposed to *B. longum* **35624** or its isogenic derivative sEPS^{neg} (n=3, 50 bacteria:1 MDDC) . Statistical significance was determined using two-way ANOVA (*p<0.05 *B. longum* **35624** versus the sEPS^{neg} strain).

Figure 4. sEPS^{neg} is not protective in a T cell transfer colitis model

Following receipt of $CD4^+CD25^-CD45RB^{hi}$ T cells, C.B-17 SCID mice were orally administered *B. longum* **35624** (n=8), sEPS^{comp} (n=8) or sEPS^{neg} (n=8) strains. (A) Weight loss and disease activity were monitored over time. Statistical significance was determined using two-way ANOVA (*p<0.05). (B) Following euthanasia, the colon:body weight ratio was determined. A representative picture of colons from *B. longum* **35624** or sEPS^{neg} –treated animals is provided. (C) The percentage of IL-17^+, IFN-γ^+ and IL-10^+ lymphocytes from mesenteric lymph nodes are illustrated (n=8 per group). Data are presented as box-and-whisker plots with the median value and max/min values illustrated. Statistical significance was determined using the Kruskal–Wallis test and Dunn's multiple comparison test (*p<0.05 sEPS^{neg} strain versus the other strains).

Figure 5. sEPS^{neg} promotes T_H17 responses in the lung

Non-sensitized animals received an OVA aerosol challenge and were intranasally administered PBS (Control, n=8). Sensitized animals received an OVA aerosol challenge and were intranasally administered PBS (OVA, n=8), or intranasally administered *B. longum* **35624** (OVA & 35624, n=8), or intranasally administered sEPS^{neg} (OVA & sEPS^{neg}, n=8). (A) The percentage of IL-17$^+$ CD3$^+$CD4$^+$ T lymphocytes, isolated from lung tissue, and secretion of IL-17 from isolated lung cells re-stimulated *ex vivo* with OVA or LPS. Similarly, IFN-γ$^+$ and IL-10$^+$ CD3$^+$CD4$^+$ T lymphocytes and *ex vivo* IFN-γ and IL-10 secretion were quantified using identical methods, (B) and (C) respectively. Data are presented as box-and-whisker plots with the median value and max/min values illustrated. Statistical significance was determined using the Kruskal–Wallis test and Dunn's multiple comparison test (*$p<0.05$ compared to the OVA group).

767 **Table 1.** Bacterial strains and plasmids used in this study.

Strain or plasmid	*Relevant characteristics*	*Reference or source*
Strains		
E. coli EC101	Cloning host, repA$^-$, Km^r	Law *et al*., 1995 (26)
E. coli XL1blue	Cloning host, , Tet^r	Stratagene
E. coli EC101 pNZ-M.1185	*E. coli* EC101 harbouring pNZ-M.1185	This study
B. longum 35624	Parent strain	Alimentary Health
sEPS^{neg}	*B. longum* **35624** harbouring insertion mutation in priming glycosyl transferase encoding gene, pgt_{624}	This study
sEPS^{comp}	sEPS^{neg} harbouring pBC1.2_pgt_{624}+*BI0343*	This study
Plasmids		
pNZEm	Gene expression vector, Em^r	Margolles *et al*., 2006 (56)
pORI19	Em^r, repA$^-$, ori$^+$, cloning vector	Law *et al*., 1995 (25)
pORI19*tet(w)_pgt*	pORI19 harbouring internal fragment of *BI0342 (pgt) and tetW gene*	This study
pBC1.2	*E. coli* –Bifidobacterial shuttle vector	Álvarez-Martín *et al*., 2007 (27)
pBC1.2_pgt_{624}+*BI0343*	pBC1.2 harbouring the cotranscribed genes pgt_{624}+*BI0343* under the control of their native promoter	This study
pNZ-M.1185	*BI1185* (*M.1185*, isoschizomer of M.EcoRII) cloned with its own promoter in pNZEM	This study

768

769

770 **Table 2.** Oligonucleotide primers used in this study are described.

Purpose	***Primer***	***Sequence***[a]
Cloning of M.**1185** in pNZEm	BI1185F_PstI	GA**CTGCAG**GCCCACTAGGTAACCAAACG
	BI1185R_SpeI	GCGC**ACTAGT**CTAGAGCAAAGCCAGTATAG
Cloning of internal 583 bp fragment of *pgt* in pORI19	BI0342F_HindIII	GAT**AAGCTT**GCGTCGGCAACTCAACTACC
	BI0342R_XbaI	GAT**TCTAGA**CGTCGGCGTTCACTACCATC
Cloning of pgt_{624}+*BI0343* in pBC1.2	BI0342FSalI	GAC**GTCGAC**ACTCCACTCTCGCTGATCG
	BI0343EcoRI	GGC**GAATTC**TAATCAACCAAGGGGGTCTG

771 [a] Restriction sites incorporated into oligonucleotide primer sequences are indicated in bold

Figure 1

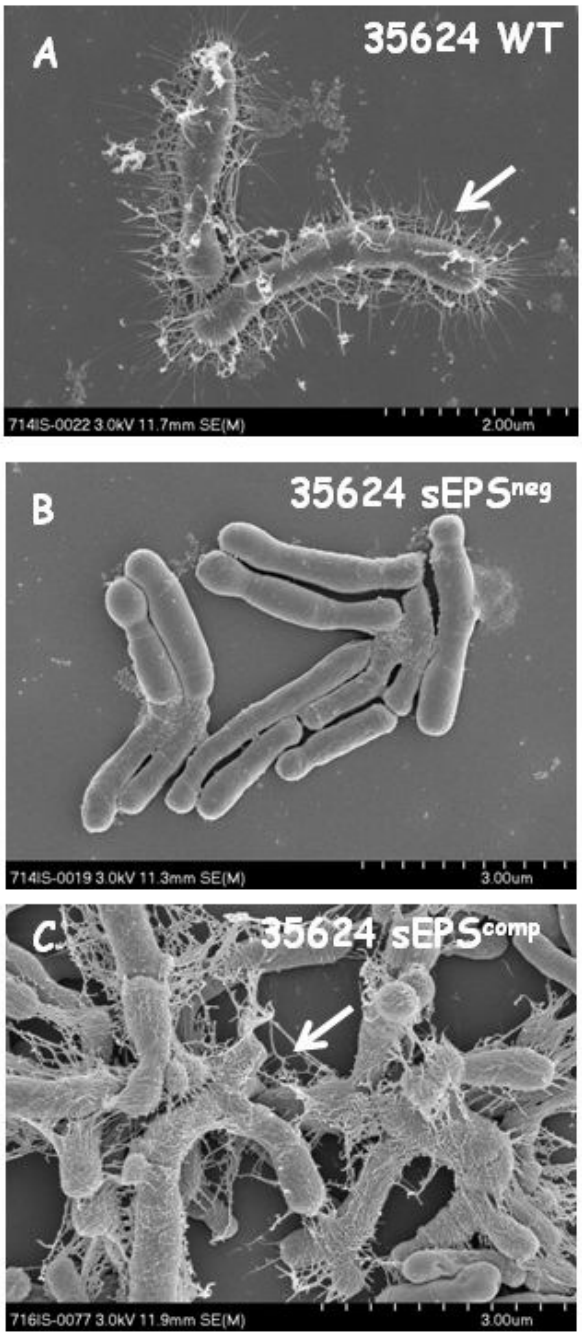

Figure 1. *B. longum* **35624** electron microscopy
Representative scanning electron microscopy (SEM) images for the *B. longum* **35624** parent strain (A, upper panel) and its isogenic derivatives, sEPS^{neg} mutant (B, middle panel) and sEPS^{comp} mutant (C, bottom panel) are illustrated. Arrows indicate the 'stringy' layer of extracellular polysaccharide visible on the *B. longum* **35624** parent strain and sEPS^{comp} strain. Scale bars are indicated at the bottom right of each panel.

Figure 2

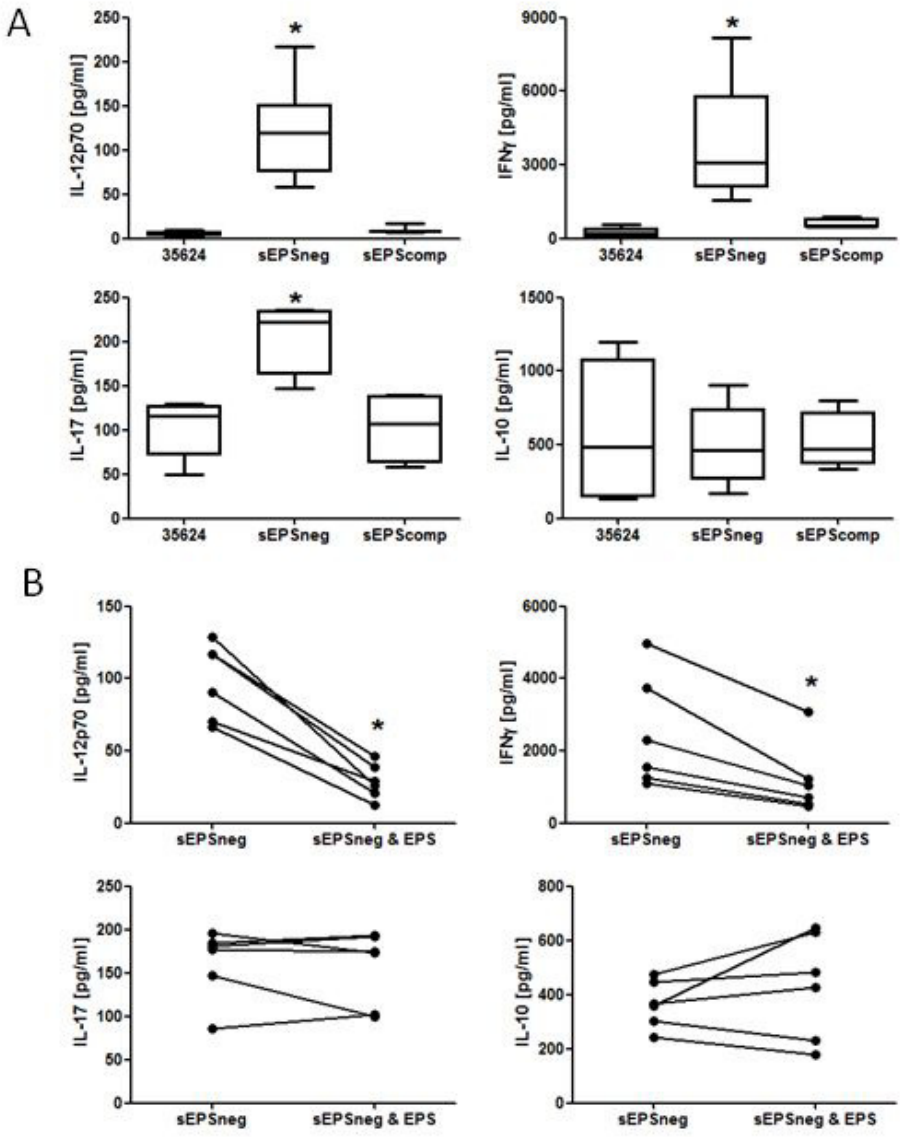

Figure 2. PBMC cytokine response to bacterial strains
(A) PBMCs from 6 healthy donors were stimulated with *B. longum* **35624** or its isogenic derivatives sEPS^{neg} or sEPS^{comp} (50 bacteria:1 PBMC) for 24 hours and cytokine secretion into the culture supernatant was quantified. Data are presented as box-and-whisker plots with the median value and max/min values illustrated. Statistical significance was determined using the Kruskal–Wallis test and Dunn's multiple comparison test (*$p<0.05$). (B) Effect of adding isolated exopolysaccharide on sEPS^{neg} strain-induced PBMC secretion of IL-12p70, IFN-gamma, IL-17 and IL-10. Each line connects the data from the same donor. The Mann–Whitney U test was used for the statistical analysis (*$p<0.05$ versus the sEPS^{neg} strain alone).

Figure 3

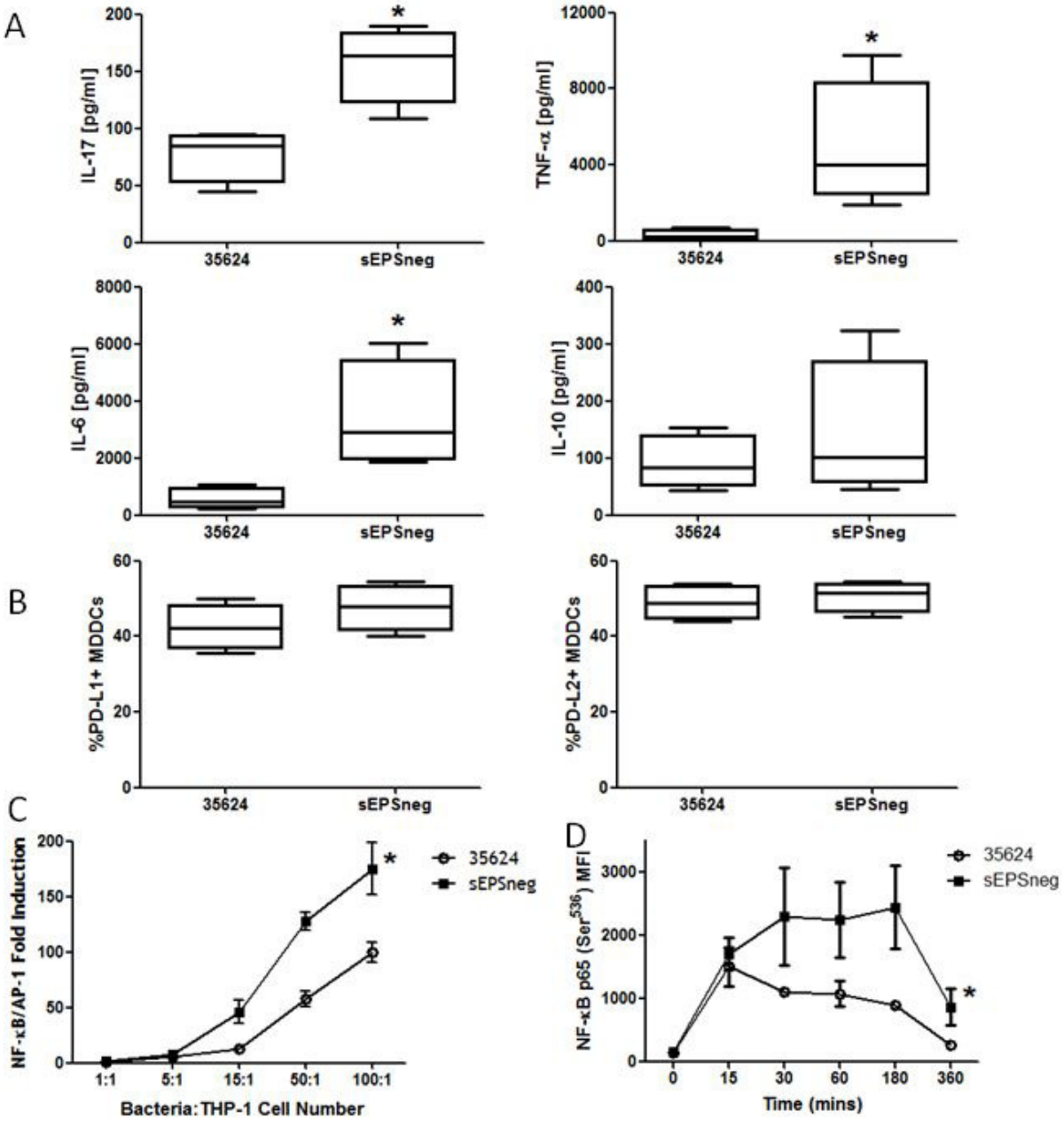

Figure 3. MDDC response to bacterial strains

MDDCs were generated from 4 healthy donors and were stimulated with *B. longum* **35624** or its isogenic derivative sEPS^{neg} (50 bacteria:1 MDDC) for 24 hours. Cytokine secretion into the culture supernatant (A) and cell surface expression of the inhibitory molecules PD-L1 or PD-L2 (B) were quantified. Data are presented as box-and-whisker plots with the median value and max/min values illustrated. The Mann–Whitney U test was used for the statistical analysis (*$p<0.05$ *B. longum* **35624** versus the sEPS^{neg} strain). (C) THP-1 NF-kB activation following exposure to increasing concentrations of *B. longum* **35624** or its isogenic derivative sEPS^{neg} (n=4 experimental replicates). (D) Activation of NF-κB in MDDCs exposed to *B. longum* **35624** or its isogenic derivative sEPS^{neg} (n=3, 50 bacteria:1 MDDC). Statistical significance was determined using two-way ANOVA (*$p<0.05$ *B. longum* **35624** versus the sEPS^{neg} strain).

Figure 4

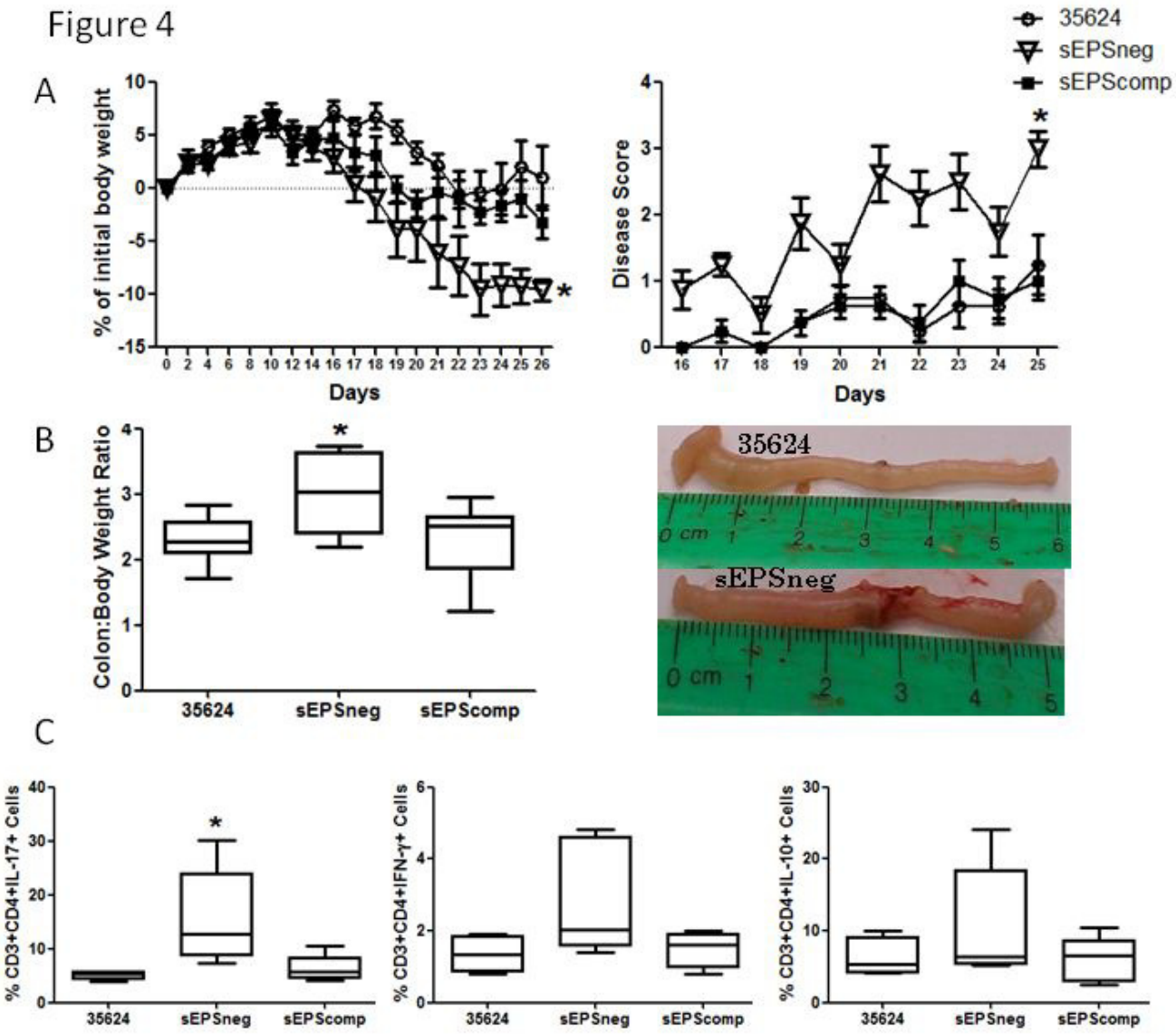

Figure 4. sEPS^{neg} is not protective in a T cell transfer colitis model
Following receipt of CD4$^+$CD25$^-$CD45RB^{hi} T cells, C.B-17 SCID mice were orally administered *B. longum* **35624** (n=8), sEPS^{comp} (n=8) or sEPS^{neg} (n=8) strains. (A) Weight loss and disease activity were monitored over time. Statistical significance was determined using two-way ANOVA (*$p<0.05$). (B) Following euthanasia, the colon:body weight ratio was determined. A representative picture of colons from *B. longum* **35624** or sEPS^{neg} –treated animals is provided. (C) The percentage of IL-17$^+$, IFN-g$^+$ and IL-10$^+$ lymphocytes from mesenteric lymph nodes are illustrated (n=8 per group). Data are presented as box-and-whisker plots with the median value and max/min values illustrated. Statistical significance was determined using the Kruskal–Wallis test and Dunn's multiple comparison test (*$p<0.05$ sEPS^{neg} strain versus the other strains).

Figure 5

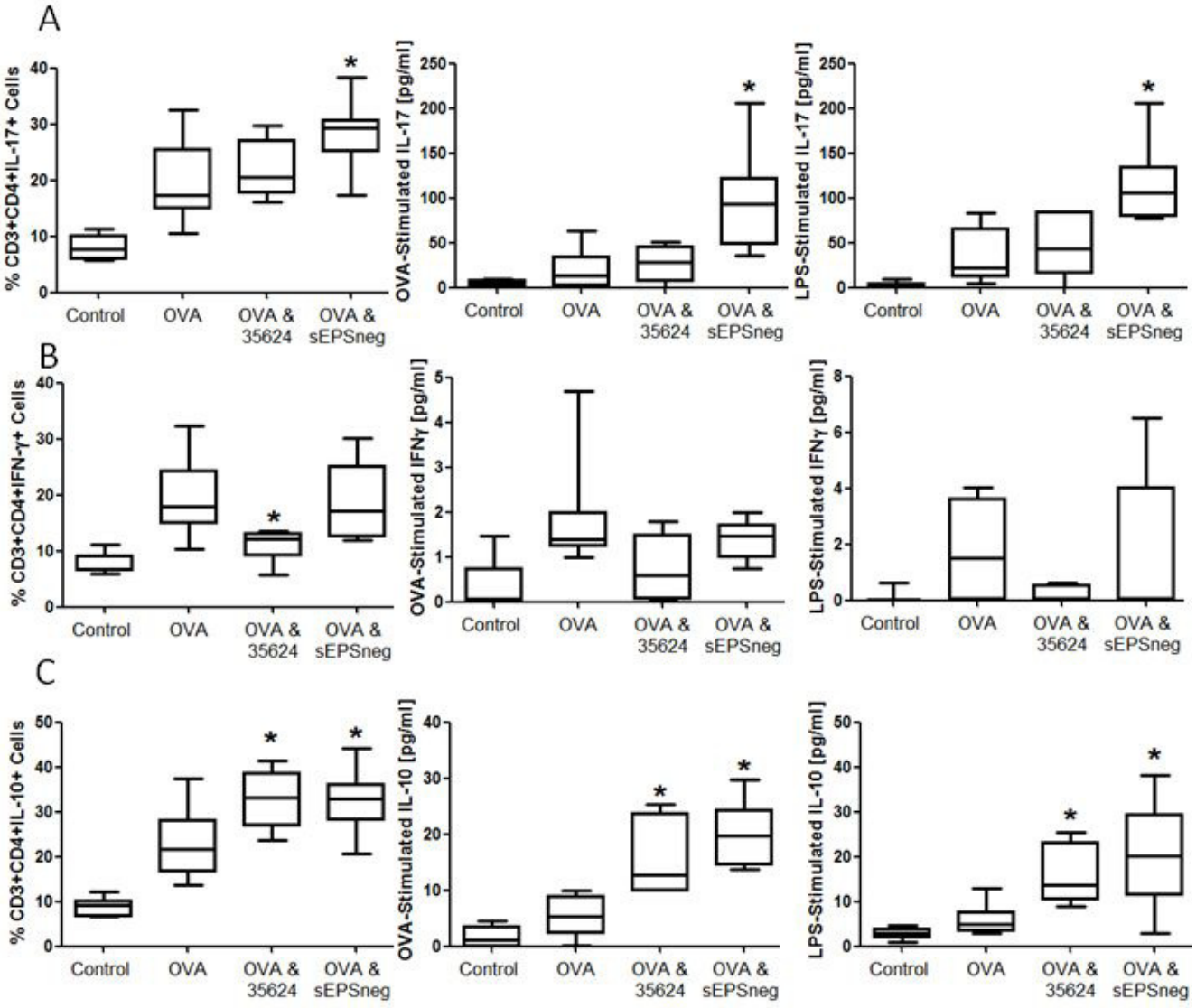

Figure 5. sEPS^{neg} promotes T_H17 responses in the lung

Non-sensitized animals received an OVA aerosol challenge and were intranasally administered PBS (Control, n=8). Sensitized animals received an OVA aerosol challenge and were intranasally administered PBS (OVA, n=8), or intranasally administered *B. longum* **35624** (OVA & 35624, n=8), or intranasally administered sEPS^{neg} (OVA & sEPS^{neg}, n=8). (A) The percentage of IL-17$^+$ CD3$^+$CD4$^+$ T lymphocytes, isolated from lung tissue, and secretion of IL-17 from isolated lung cells re-stimulated *ex vivo* with OVA or LPS. Similarly, IFN-g$^+$ and IL-10$^+$ CD3$^+$CD4$^+$ T lymphocytes and *ex vivo* IFN-g and IL-10 secretion were quantified using identical methods, (B) and (C) respectively. Data are presented as box-and-whisker plots with the median value and max/min values illustrated. Statistical significance was determined using the Kruskal–Wallis test and Dunn's multiple comparison test (*$p<0.05$ compared to the OVA group).